RAD Conference Proceedings, vol. 6, pp. 15–20, 2022
ISSN 2466-4626 (online) | DOI: 10.21175/RadProc.2022.03
www.rad-proceedings.org

METHOD OF SETTING OPTIMAL OPERATING VOLTAGE FOR RADIATION DETECTORS CONTAINING THIN PLASTIC SCINTILLATORS

Aleš Jančář[1*], Jiří Čulen[1], Filip Mravec[1], Zdeněk Matěj[2]

[1]VF, a.s., Černá Hora, Czech Republic
[2]Masaryk University, Brno, Czech Republic

Abstract. *In this paper, we discuss the method of setting the optimal working voltage on the photomultipliers of detectors containing thin plastic scintillation materials. These plastic scintillators may additionally include a zinc sulfide ZnS(Ag) layer for the separation of alpha and beta particles. The ionizing radiation on the thin plastic scintillators is not fully absorbed and therefore it is not possible to determine the position of the Compton edge. This is very important for energy calibration. We have proposed a simple method for this purpose and carried out all tests with the newly developed smart frisking probe. The results are presented.*

Keywords: *thin plastic scintillator, plateau measurement, compton edge, high voltage, sensitivity, MCNP*

1. INTRODUCTION

The thin plastic scintillators are widely used ranging from portable devices to radiation spectrometers. They can be used as pulse counters or can be set using the sensitivity (cps/Bq) to determine the activity [Bq] or specific activity value [Bq/cm^2] for a given radionuclide. In order to determine sensitivity, the optimal high voltage must be set on the photomultipliers of radiation detectors.

Each radiation detector has a typical sensitivity. The value of sensitivity mainly depends on the type of detector, high voltage, low and high level of discrimination. If we use spectrometric detectors, for example, NaI(Tl) or YAP(Ce) crystals we can set a low and high level of discrimination according to the request of energy range (for example 100 keV to 3 MeV). The electronic part of the detector MCA (Multi Channel Analyzer) has a specific number of channels (for example 1024 channels). Easily we can calculate the number of keV/channel. For measurement we used radiation source of Cs-137 (662 keV). According to the number of keV/channel we calculate a specific channel for the peak of Cs-137. We adjusted high voltage for the specific channel (Cs-137) and carried out measurement of sensitivities.

How can we set the optimal high voltage on the non-spectrometric detector with plastic scintillators? During the development of the detectors, we encountered this problem and invented a method for setting optimal operating voltage. This method provides the same energy calibration on the detectors with plastic scintillators.

2. DEFINITION AND PRINCIPLE

Ionizing radiation hitting certain materials can produce optical photons (scintillation). The existence of luminescence centers is a necessary condition for scintillation. These are created by the insertion of extraneous ions into a crystal lattice. Doped scintillators are created this way, e.g., ZnS(Ag), ZnS(Cu) or NaI(Tl).

The electronic structure can be divided into energy levels - singlets (S_0, S_1, S_2 ...) and energy levels - triplets (T_1, T_2, T_3 ...). Molecular atoms used in these kinds of detectors have spacing between S_0 and S_1 approximately 3 to 4 eV. Gaps become smaller for higher levels.

Electrons can jump to higher energy states as a result of the absorption of kinetic energy from charged particles. Electrons in higher states de-excite to state S_1 within picoseconds.

States with higher vibrational energy are not in thermal equilibrium with the surrounding molecular atoms and quickly lose their energy surplus. The effect of excitation in organic scintillators is that a population of excited molecular atoms is created on level S_{10} in a short time.

Prompt fluorescence is radiated during the transition between energy level S_{10} and vibrational levels S_0 of the electron ground state. For most organic scintillators the time constant for prompt fluorescence is in nanoseconds.

Delayed fluorescence occurs during the transition from a higher energy state into a lower one. A triplet state can be created during a transient state of certain excited states. The mean lifetime of energy state T_1 is much longer than the mean lifetime of energy levels. This postponed de-excitation leads to delayed fluorescence within milliseconds, see Fig. 1.

* ales.jancar@vfnuclear.com

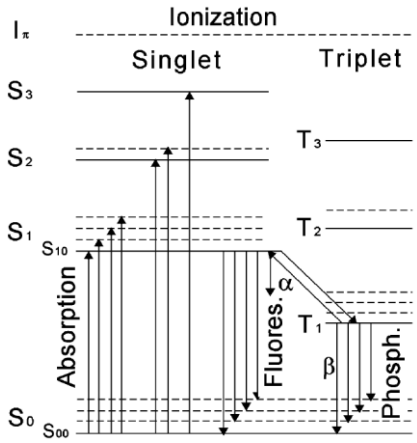

Figure 1. Transition scheme for the excitations and de-excitations in an organic scintillator [7].

2.1. Detection Principle of Scintillators

The scintillation principle is one of the oldest ways to detect alpha, beta, gamma and neutron particles. Photons are created when the ionizing particle interacts with the scintillator. Because the direction of these photons is random, the scintillator is surrounded by a white reflective coating. This improves the light collection in the PMT. These incident photons hit the photocathode, which ejects electrons due to the photoelectric effect. These electrons are accelerated by the high voltage between dynodes of PMT.

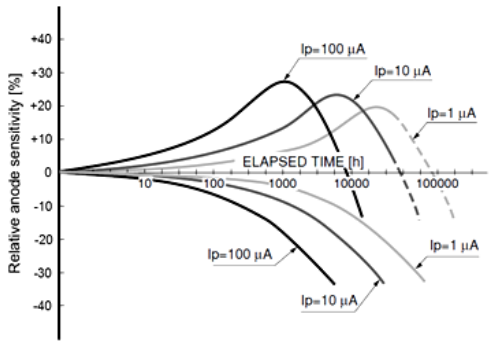

Figure 2. Typical anode current dependence of photomultiplier in time [6].

The impact of the accelerated electrons on the dynodes creates the emission of more electrons (secondary emission). The connected working resistor creates voltage pulses that are processed electronically. The stability of the photomultiplier depends on the anode current as well as the material of the photocathode and dynodes. Figure 2 shows a typical dependence of the anode current on time.

The developed detector prototype shows anode current < 1 microampere, i.e., long stability. However, if the PMT is not used for several months, its properties may return to the state before the warming up.

3. Characteristics of the Plastic Scintillator

The plastic scintillators without the ZnS(Ag) layer are not suitable for alpha/beta separation due to the close similarity between alpha and beta impulses. On the other hand plastic scintillators coated with the ZnS(Ag) layer thick enough can stop incident alpha particles while allowing the low energy beta radiation to pass, e.g., C-14.

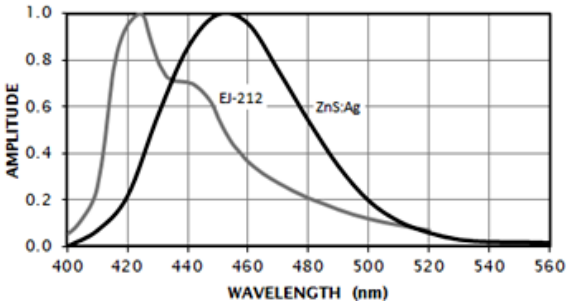

Figure 3. Typical anode current dependence of photomultiplier in time [6].

We used a thin plastic scintillator of the EJ-444 type from Eljen Technology. This scintillator is specially formulated for applications including industrial and health physics measurements of alpha, beta, gamma, and neutron radiation.

Table 1. The parameters of plastic scintillator EJ-212 coated ZnS(Ag) [8].

Properties	EJ-212	ZnS(Ag)
Light Output (% Anthracene)	65	300
The wavelength of Maximum Emission [nm]	423	450
Decay Time [ns]	2.4	200
Density [mg·cm^{-2}]	1023	-
Phosphor Density [mg·cm^{-2}]	-	3.25 ± 0.25

The scintillator EJ-444 consists of a 0.25 mm thick plastic scintillator EJ-212 coated from one side with a layer of zinc sulfide doped with silver: ZnS(Ag). Emission spectra are shown in Fig. 3 and parameters of the scintillator are stated in Table 1.

3.1. Experimental Setup and Technique

The knowledge of the scintillator's parameters (response functions, decay time, etc.) is necessary in order to set up the electronics part and separation algorithm correctly.

Experimental measurements have been performed with a two-parameter digital spectrometric system NGA-01.

Figure 4. Two-parametric digital neutron-gamma spectrometer NGA-01 [3,4].

The prototype of the radiation detector has been connected to the NGA-01 input (Fig. 4). The input analog signal from the detector is digitized by two fast ADC converters working with a sampling frequency of 500 MHz. Digital signal processing is implemented in FPGA Xilinx Virtex-6. FPGA is able to process all data flowing from both ADCs (24 Gbits per second). The ADC output is processed by the FPGA with a speed of 24 GB/s.

3.1.1 Dependence of Pulses Amplitude on the Radiation Energy

The following list of radiation sources has been used for experimental measurements. Surface activities of the sources have been approx. 20 Bq/cm². Senstive area of the detector was placed directly on the sources. Measurement time was set to 100 s.

The reference amplitude spectra for radiation sources Cl-36 and Am-241 are presented, see Fig. 5 and Fig. 6. The levels of a comparator (mV) are shown on the x-axis and pulses per second (cps) from the detector are shown on the y-axis.

The alpha sources have a higher level of ionization than beta sources. This was verified by measurements. According to the results of the measurements (Fig. 5 and Fig. 6), the comparator level of the radiation detector has been set to 80 mV for the alpha channel and 40 mV for the beta channel.

Table 2. The list of radiation sources.

Radionuclide	Radiation type	Eα [MeV]	Eβ max [keV]	Eγ [keV]
^{14}C	β	-	156.5	-
^{36}Cl	β	-	709.6	-
^{60}Co	β, γ	-	317.1	1 173; 1 132.5
^{90}Sr/^{90}Y	β	-	546.0 / 2 283.9	-
^{137}Cs	β, γ	-	513.9	661.7
^{204}Tl	β	-	763.4	-
^{239}Pu	α	5.2	-	-
^{241}Am	α, γ	5.5	-	59.5

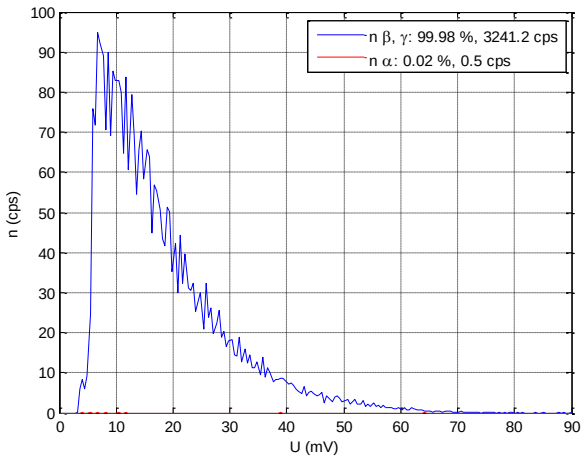

Figure 5. Dependence of pulses amplitude of ^{36}Cl.

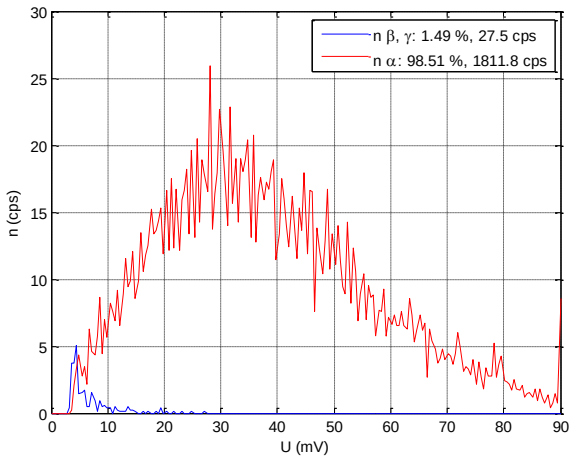

Figure 6. Dependence of pulses amplitude of ^{241}Am.

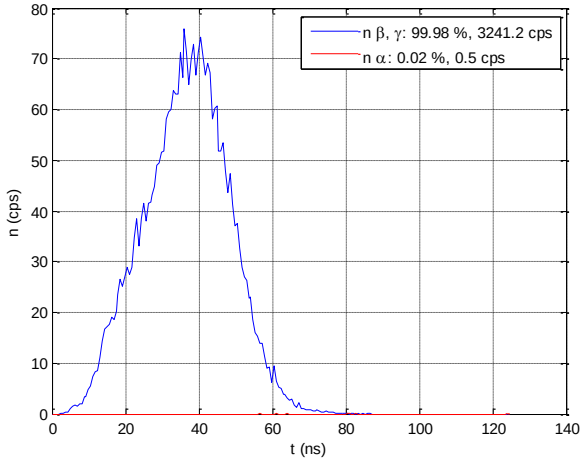

Figure 7. Dependence of pulses decay time of ^{36}Cl.

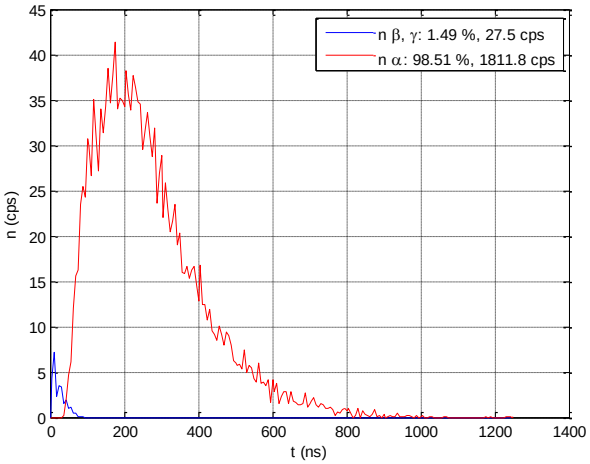

Figure 8. Dependence of pulses decay time of ^{241}Am.

3.1.2. Dependence of the Pulses Decay Time on Radiation Energy

Experimental measurements with the radiation sources Cl-36 and Am-241 have been performed. Information about radiation sources are stated in

Table 2. The waveforms of the pulses from the detector have been processed, see Fig. 7 and Fig. 8. According to the following formula decay time has been calculated:

$$V(t) = V_0 e^{\frac{-t}{\tau}}, \text{ where} \qquad (1)$$

$V_{(t)}$ – value in the time (t);

V_0 – initial value;

T – time;

τ – decay time.

The calculated decay time for beta radiation (Cl-36) is 2.8 ns and the decay time for alpha radiation (Am-241) is 180 ns. Measurement results of the decay times have been verified with the producer's data stated in Table 1.

4. Process of the Setting Optimal Operating Voltage

Process of the setting up the optimal working voltage is problematic with non-spectrometric scintillators. Ionizing radiation is not fully absorbed in the thin scintillator thus is difficult to determine the Compton edge.

The developed simple method contains two steps:

1. Plateau measurement;
2. Optimal working voltage calculation.

4.1. Experimental Setup

The prototype of the alpha/beta radiation probe has been used for testing, see Fig. 9.

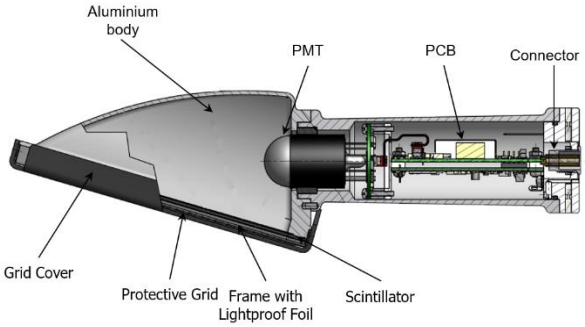

Figure 9. The prototype of the alpha/beta radiation probe.

The mechanical construction of the radiation probe has been designed for maximum light collection from the surface inside the detector. The maximum wavelength from the scintillator corresponds to the maximum wavelength of the photomultiplier.

The probe housing (body and handle) is made of aluminum. The rectangular frame of the body contains a 0.25 mm thick plastic scintillator EJ-444 which is protected by aluminum reflector and a protective metal grid. The handle of the probe contains PMT with an active voltage divider, electronics part and connector for communication and power supply.

4.2. Plateau Measurement

The process of plateau measurement is a dependence sensitivity (cps/Bq) of the radiation probe to high voltage (V). Radionuclide of energy 59.5 keV (Am-241) has been used for the plateau measurement. By derivation of the alpha plateau curve, we can find the inflection point corresponding to the energy of the particle whose trajectory is most likely to pass through the scintillator.

4.2.1. Plateau Measurement Procedure

The plateau measurement procedure contains the following steps:

1. Set the level discrimination (LLD1) to 40 mV;
2. Set the counting time to 60 s;
3. Set a high voltage step of 10 V in the range of 290 V to 550 V;
4. Carry out the measurement of background count rate n_{bg} (cps) for each set high voltage;
5. Place a surface radiation source of ^{241}Am directly on the probe's protective grid;
6. Carry out count rate n_s (cps) measurement with a source for each set high voltage;
7. Calculate sensitivities R (cps/Bq) according to the following formula:

$$R = \frac{n_{net}}{A} = \frac{n_s - n_{bg}}{A_{\text{Ref}} \times 2^{\frac{(t_{end} - t_{start})}{T_{1/2}}}} \left[\frac{cps}{Bq}\right], \qquad (2)$$

n_{net} - net count rate [cps];

A - activity to date of measurement [Bq];

A_{ref} - reference activity [Bq];

t_{start} - date and time of measurement start [yy-mm-dd hh:mm:ss];

t_{end} - date and time of measurement end [yy-mm-dd hh:mm:ss];

$T_{1/2}$ - half-life [days].

8. Crate a graph of sensitivity to high voltage;
9. Carry out the derivation of the alpha plateau curve;
10. Calculate the inflection point corresponding to the high voltage HV_1, see Fig. 10.

4.3. Calculation of the Optimal Operating Voltage

The high voltage HV_1 and LLD_1 parameters have been determined in section 4.2.

Set the level of comparator LLD_2 to the end of the measured plateau, see Fig. 10. The operating high voltage HV_2 for the radiation probe can be calculated using to the following formula:

$$HV_2 = HV_1 \left(\frac{LLD_2}{LLD_1}\right)^{\frac{1}{\alpha \times N_{dyn}}}, \qquad (3)$$

where HV_1 - high voltage corresponds with an inflection point;

LLD_1 - level of comparator corresponds with HV_1;

LLD_2 - level of comparator corresponds with HV_2;

α - dynode voltage amplification coefficient [6];

N_{dyn} - number of PMT dynodes.

4.4. Voltage Amplification Coefficient

The dynode voltage amplification coefficient is a constant for each type of photomultiplier. Usually they are specified in a datasheet of photomultiplier producers.

We carried out verification of the amplification coefficient for the photomultiplier type 9114FLB, ET Enterprises. We used the results of the measurements stated in sections 4.2, 4.3. and calculated the value of the voltage amplification coefficient according to the following formula.

$$\frac{LLD_2}{LLD_1} = \left(\frac{HV_2}{HV_1}\right)^{\alpha.N_{dyn}} \Rightarrow \alpha = \frac{1}{N_{dyn}} . \frac{\log\left(\frac{LLD_2}{LLD_1}\right)}{\log\left(\frac{HV_2}{HV_1}\right)} \quad (4)$$

5. Results and Discussion

A graph of sensitivity versus high voltage was created for the radiation probe. The graph is shown in Fig. 10, the parameters of high voltage, inflection point and low level discrimination are marked.

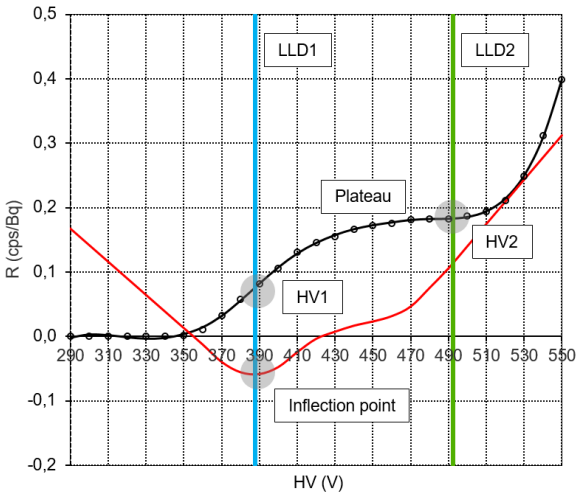

Figure 10. Plateau of alpha/beta radiation probe with radionuclide ^{241}Am.

The dynode voltage amplification coefficient has been verified, see Fig. 11. The value specified by the manufacturer of PMT type 9114FLB is 0.81. The experimentally determined value of the α amplification coefficient is 0.809.

The sensitivity parameters have been verified by Monte Carlo simulations using the code MCNP ver. 6.2, see Table 3. There is a good agreement between measurements and simulations.

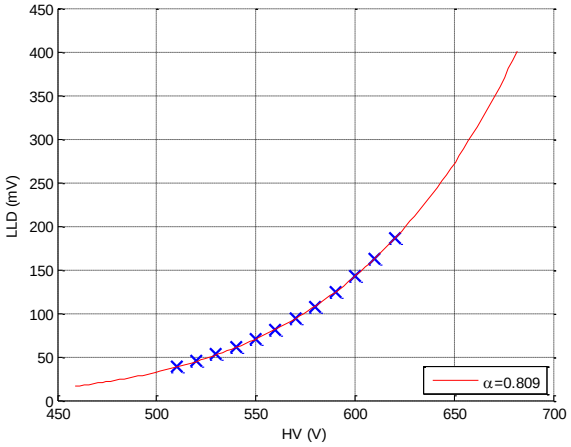

Figure 11. The measurement of voltage amplification coefficient with radionuclide ^{241}Am.

Table 3. The comparison of Monte Carlo simulations with measurement.

Radionuclide	MC sensitivity simulation [cps/Bq]	MC efficiency simulation [%]	Measured sensitivity [cps/Bq]	Measured efficiency [%]
^{14}C	0.09	15	0.08	13
^{36}Cl	0.32	51	0.33	51
^{60}Co	0.21	33	0.19	30
^{90}Sr/^{90}Y	0.35	51	0.34	50
^{137}Cs	0.32	43	0.32	43
^{204}Tl	0.29	44	0.27	41
^{239}Pu	0.20	40	0.19	38
^{241}Am	0.22	44	0.21	44

6. Conclusion

A newly developed alpha/beta radiation probe has been tested and adjusted according to the presented method. Using this method we are able to guarantee the same energy calibration in the energy range of 150 keV to 3 MeV.

This method can be used for all types of radiation detectors containing alpha/beta sensitive plastic scintillators.

References

1. S. Hohara et al., "A simple method of energy calibration for thin plastic scintillator," *IEEE Transactions on Nuclear Science,* vol. 48, no. 4, pp. 1172–1176, Aug. 2001. https://doi.org/10.1109/23.958745
2. N. Kudomi, "Energy calibration of plastic scintillators for low energy electrons by using Compton scatterings of rays," *Nuclear Instruments and Methods in Physics Research Section A: Accelerators, Spectrometers, Detectors and Associated Equipment,* vol. 430, no. 1, pp. 96–99, Jun. 1999. https://doi.org/10.1016/S0168-9002(99)00200-4
3. G. Knoll, "Scintillation Detector Principles," in *Radiation Detection and Measurement*, 4th ed., Danvers (MA), USA: John Wiley & Sons, 2010, ch. 8, pp. 223–275. Retrieved from: https://www-f9.ijs.si/~golob/sola/seminar/scintilatorji/Leo.pdf

Retrieved on: Jun. 15, 2022
4. P. Nicholson, "Pulse Shaping Methods for Spectrometry" in *Nuclear Electronics*, Norwich, UK: John Wiley & Sons, 1974, ch. 3, pp. 88–95.
5. M. Veškrna et al., "Digitalized two parametric system for gamma/neutron spectrometry," in *Proc. ANS RPSD 2014 – 18th Topical Meeting of the Radiation Protection and Shielding Division,* Knoxville (TN), USA, 2014.
Retrieved from:
https://is.muni.cz/repo/1210637/RPSD2014_-_Digitalized_two_parametric_system_for_gammaneutron_spectrometry.pdf
Retrieved on: Jun. 15, 2022
6. M. Pavelek et al., "Fast digital spectrometer for mixed radiation fields," in *Proc. 2017 IEEE Sensors,* Glasgow, UK, 2017, pp. 1–3.
https://doi.org/10.1109/ICSENS.2017.8234012
7. J. Gerndt, *Detektory ionizujícího záření*, 1. vyd., Praha, Česká republika, Vydavatelství ČVUT, 1996.
(J. Gerndt, *Ionizing Radiation Detectors*, 1st ed., Prague, Czech Republic, Czech Technical University Press, 1996.)
8. S. Flyckt, C. Marmonier, *Photomultiplier tubes: Principles & applications*, Brive, France, Photonis, 2002.
Retrieved from:
https://www2.pv.infn.it/~debari/doc/Flyckt_Marmonier.pdf
Retrieved on: Dec. 6, 2022
9. M. Höök, "Study of the pulse shape as a means to identify neutrons and gammas in a NE213 detector," diploma thesis, Uppsala University, Department of Neutron Research, Uppsala, Sweden, 2006.
Retrieved from:
https://www.diva-portal.org/smash/get/diva2:342845/FULLTEXT01.pdf
Retrieved on: Dec. 6, 2022
10. Plastic Scintillators Database, Eljen Technology, Sweetwater (TX), USA.
Retrieved from:
https://eljentechnology.com
Retrieved on: Dec. 6, 2022